Effect of the cooling rate on encapsulant's crystallinity and optical properties, and photovoltaic modules' lifetime

Vincent Meslier, Bertrand Chambion, Amandine Boulanger, Ichrak Rahmoun, Fabien Chabuel, Timea Bejat

EPJ Photovoltaics **14**, 2 (2023)

https://doi.org/10.1051/epjpv/2022028

Special Issue on 'WCPEC-8: State of the Art and Developments in Photovoltaics', edited by Alessandra Scognamiglio, Robert Kenny, Shuzi Hayase and Arno Smets

Available online at: www.epj-pv.org

REGULAR ARTICLE

OPEN ACCESS

Effect of the cooling rate on encapsulant's crystallinity and optical properties, and photovoltaic modules' lifetime

Vincent Meslier*, Bertrand Chambion, Amandine Boulanger, Ichrak Rahmoun, Fabien Chabuel and Timea Bejat

CEA INES, Solar Technologies Department, Le Bourget-du-Lac, France

Received: 30 June 2022 / Received in final form: 20 October 2022 / Accepted: 18 November 2022

Abstract. Since the renewable energy thrive, performances and lifetime of photovoltaic (PV) modules have been one of the big international concern. The mechanical bonding between the different components and the materials' choice can significantly improve both performances and lifetime of PV modules. The manufacturing process plays also a significant part in the modules lifetime [G. Oreski, B. Ottersböck, A. Omazic, Degradation Processes and Mechanisms of Encapsulants, in Durability and Reliability of Polymers and Other Materials in Photovoltaic Modules (Elsevier, 2019), pp. 135–152]. This work deals with the controlled cooling part of the manufacturing process. The aim is to characterize its influence on an encapsulant properties, and its influences on modules degradation. This work is a part of improving both performances and lifetime of PV modules. First, the work focuses on describing the real temperature seen by a thermoplastic polyolefin encapsulant during the lamination process. A multi-chamber R&D laminator is used and studied in order to better know the industrial equipment. Results show that the cooling process reduces the time to cool down by a factor of ~5 compared to natural air convection. Secondly, the material's micro-structure is analysed by Differential Scanning Calorimetry (DSC). The impact of the process is quantified. It does have an influence on the encapsulant crystallites' size distribution without modifying the total crystallinity. Thirdly, the impact of the cooling process on optical properties is investigated. Using spectrophotometry and haze-metry optical characterization, coupled with a known light spectrum, the light intensity coming out from the material is analysed. Results show that the cooling process does not have any influence on transmittance nor reflectance. However, a 34% reduction in the haze factor is recorded when using the industrial laminator cooling process. Fourthly, mechanical bond strength between glass and encapsulant is characterized over ageing. Normalized 10 mm width strips are used to estimate the bond strength. It demonstrates that applying pressure during cooling does not influence the bond strength between glass and encapsulant after 1000 h of damp heat ageing. Finally, impact of the cooling process over ageing on PV modules is discussed. Two accelerating ageing methods, 300 Thermal Cycles and 1000 h damp heat, are used to speed up ageing processes. The electrical components of the PV modules are analysed and used to assess the modules' degradation. Modules manufactured with the cooling process are more sensitive to damp heat after 500 h than modules cooled by natural convection. No significant differences were found in thermal cycling ageing.

Keywords: Post-crystallisation / thermoplastic polyolefin (TPO) / differential scanning calorimetry (DSC) / bonding strength / ageing

1 Introduction

To address climate change requirements, decarbonized energy sources need to be developed. Solar panels are part of the solution. In this way, a significant number of solar panels are currently manufactured. To increase production rate, a new cooling process has been developed by industrialists: the Cooling Press.

Packaging is an actual and current challenge aiming at protecting cells meanwhile optimizing photovoltaic (PV) modules' yield and ageing endurance. The classic process stacks PV cells between two glasses and two polymer sheets named encapsulant. To assemble the whole stack, a lamination process can be used. Lamination consists in heating and pressing the whole stack so as to melt the encapsulant and bond layers together (see Fig. 1). To optimize the throughput in industry, a Cooling Press step is used to cool down modules at the end of the heating process.

Beyond these considerations, we propose to focus the work on the Cooling Press consequences on encapsulant. A global approach will be assumed. From thermal characterization to ageing tests on modules, through dedicated techniques for polymer microstructure investigation (calorimetry, optical measures).

* e-mail: vincent.meslier@cea.fr

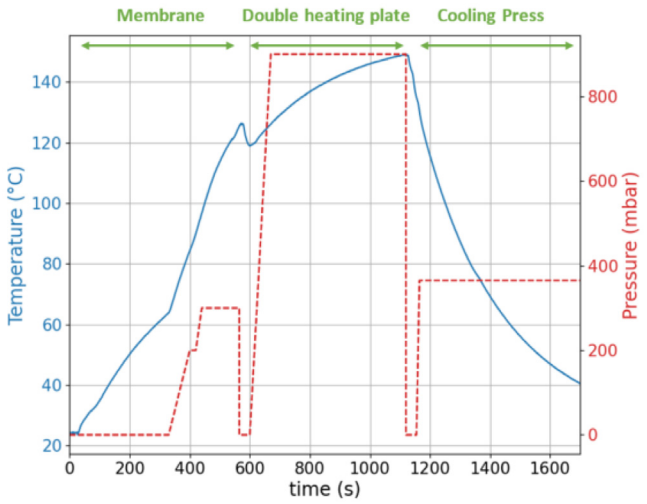

Fig. 1. Typical lamination process parameters used for Si-cells PV modules, with Cooling Press step.

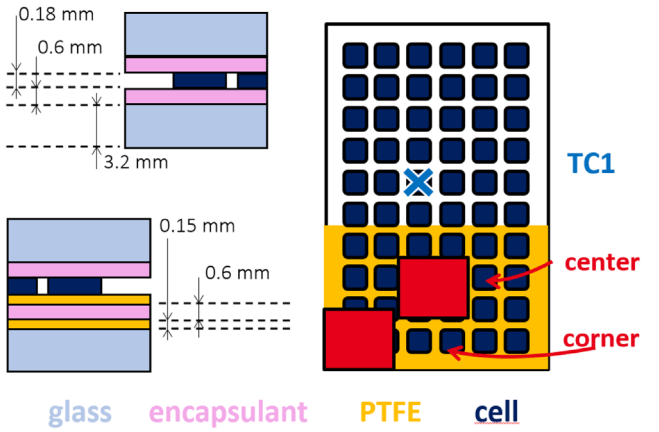

Fig. 2. Cross-section (not to scale) of the developed PV modules. It has two parts; the top one includes a thermocouple (TC1); the bottom one has two added PTFE layers. These layers allow the extraction of the encapsulant after lamination. It will be helpful for Sections 3 and 4.

A first section is presenting the cooling rate of the Cooling Press, compared to natural convection. The second section is showing the consequences of the Cooling Press on polymer crystallinity. The third section is dealing with the polymer optical changes due to the new cooling rate. The fourth section investigates the consequences on the bond strength between the encapsulant and the glass. The last section compares the ageing endurance of PV modules manufactured with and without the Cooling Press.

2 Cooling rate monitoring

In this section, the temperature monitoring set up will be first presented. An analysis of the results is following. The traditional manufacturing air cooling will be compared to the Cooling Press one. This monitoring will be used for Differential Scanning Calorimetry analysis (Sect. 3).

2.1 Method

Two instrumented glass-glass (GG) photovoltaic (PV) modules were built with a Thermoplastic Polyolefine (TPO) encapsulant, 600 µm thick. Cells have been added without electrical connections, just as thermal loads. To monitor the temperature evolution within the module, a K thermocouple has been inserted as shown on Figure 2. It has been calibrated at room temperature.

The thermocouple has been inserted between the two encapsulant layers, just above a cell. It allows to catch the temperature in the thickness center. Temperature has been recorded during the whole lamination.

The bottom part of the module is useful for Sections 3 and 4. It will be described there.

One PV module has been cooled down by natural air convection while the other dealt with the Cooling Press. Natural air convection is achieved by leaving the module on a table at controlled room temperature.

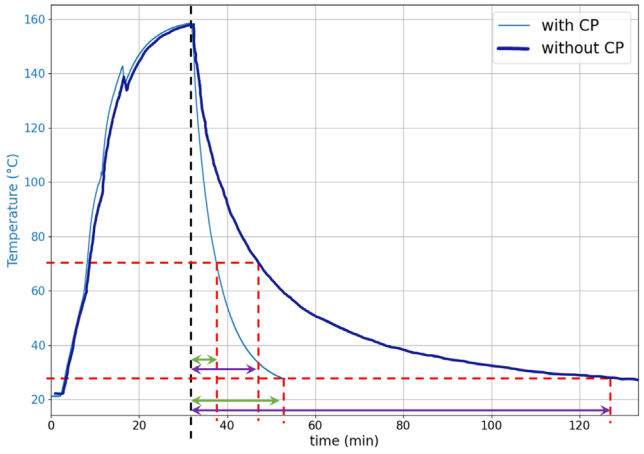

Fig. 3. Experimental temperature monitoring from TC1 with iso-thermal lines at 70 °C and 27 °C.

Table 1. Return temperature time (RTT) in the module's center for both cooling types. CP stands for Cooling Press.

	RTT70 (s)	RTT27 (s)
With CP	340	1300
Without CP	895	6065
Ratio (Without/With)	2.63	4.67

2.2 Results

The experimental temperature curves from sensor TC1 are shown on Figure 3.

From Figure 3, the return temperature time to 70 °C and 27 °C have been extracted. Return temperature time is defined as the time needed for materials to be at a specified temperature from the beginning of the cooling (black dashed line on Fig. 3). Results are summarised in Table 1.

The return temperature time at 70 °C has been chosen because below the encapsulant crystallisation temperature. The first result of this work is to show that the cooling with Cooling Press is about five-time faster than by natural convection to go to room temperature. This is equivalent to a reduction of manufacturing time by 2.5. Manufacturing time take into account the previous heating steps.

This work tries to determine what are the consequences of this fast cooling over the encapsulant's properties. The next section presents the impact of this cooling step over encapsulant's crystallinity.

3 Crystallinity analysis

This section will present Differential Scanning Calorimetry (DSC) results. Since, micro-structure can influence macroscopic properties, the idea was to explain possible macroscopic changes. The goal is to know whether the cooling rate can influence the material crystallinity.

3.1 Method

Two main experiments have been realised to study the cooling rate effect on the encapsulant crystallinity. The calorimeter is a Q20 TA instrument, calibrated with indium. Samples were kept in hermetic capsules.

For polyethylene-based polymers, such as EVA (Ethylene Vinyl Acetate) or other TPO (Thermoplastic Polyolefin) a slow formation of thin crystallites of polyethylene have been noticed [1–4]. It is a post-crystallisation at room temperature. This post-crystallisation is possible because the room temperature is far above the glass transition temperature (around −40 °C for our encapsulant). Thin crystallites appear between the larger ones which are formed during the fast cooling.

In order to study this slow effect due to chain mobility at room temperature, the following protocol has been conducted:

- Taking an encapsulant sample without any thermal history, i.e. melted at higher temperature than its fusion temperature during 15 min.
- Cooling it at 10 °C. min^{-1} to 20 °C.
- Keeping the sample at 20 °C during [0, 1, 5, 15, 30, 120, 300, 600] min.
- Once the sample has waited at controlled temperature, then cooling it at 10 °C. min^{-1} to −80 °C, and analysing it at 10 °C. min^{-1} until 160 °C.

Besides, two samples were also analysed after 14 and 35 days at room temperature. This environment was less controlled than inside the calorimeter. Temperature varied from 20 to 25 °C in the laboratory.

The second experiment has analysed encapsulant pieces that have been withdrawn from the two modules of Section 2.2. Some pieces were cooled down by natural convection while others by the Cooling Press. The pieces have been removed from two different areas − corner and center − in each module, see Figure 2.

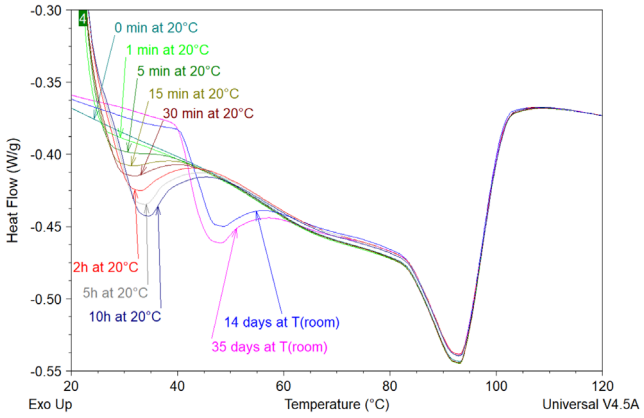

Fig. 4. DSC results of samples that have waited at 20 °C during different amounts of time before being analysed. The glassy transition temperature of the polymer is −40 °C.

Two samples from each location and cooling type have been analysed.

The material specific melting heat is obtained by integrating the melting peak. In Figure 6, this is the area between the curve and the red line. The red line is chosen to be as horizontal as possible. So as to be consistent between the experiment, the same temperature boundaries for the integration are chosen, here 22 °C and 108 °C.

From this specific melting heat, it is possible to estimate the crystallinity ($\chi(\%)$) [2,3,5] of a semi-crystalline material. This can be done using equation (1).

$$\chi(\%) \simeq \left(\frac{\Delta H_m}{\Delta H_{100}} \times 100 \right) \tag{1}$$

where ΔH_m is the specific melting heat of the sample, ΔH_{100} the specific melting heat for the 100% crystalline polymer. Our encapsulant is a polyethylene-based polymer so ΔH_{100} is the specific melting heat for 100% crystalline polyethylene (288 J. g^{-1}).

In all analysis, samples were cooled until −80 °C at 10 °C. min^{-1} (the glassy transition temperature is around −40 °C). Then, samples were heated until more than 110 °C at 10 °C. min^{-1} to catch the entire melting peak.

3.2 Results

Results from the post-crystallisation at room temperature experiments are presented on Figure 4. The time-dependent shape of the endotherm shown on Figure 4 proves the material post-crystallisation. The effect of temperature is significant as soon as a few minutes. The fact that DSC is showing an endotherm allows to speak about crystallites.

Endotherm moving from low temperature to higher ones means that there is a growth in the crystallites size. The increasing deepness' peak with time demonstrates an increasing number of crystallites [1]. Results from 14 and 35 days at room temperature are more difficult to interpret

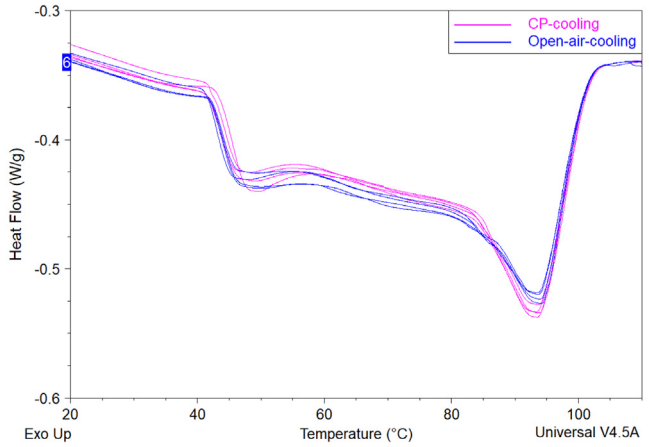

Fig. 5. DSC results for four samples of each cooling method. CP stands for Cooling Press.

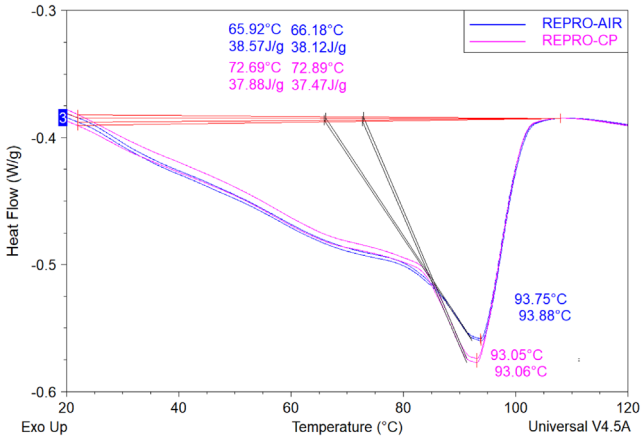

Fig. 6. DSC results for two samples of each cooling method which has been reproduced inside the calorimeter. REPRO-AIR are results from the reproduced natural convection cooling. REPRO-CP from the reproduced Cooling Press cooling.

due to the fact that they were not in a very controlled environment. Nevertheless, they confirm the clear tendency of crystallites to grow both in size and numbers with time.

This first experiment demonstrates that there is a post-crystallisation of the encapsulant at room temperature. Therefor, the next results analysis will not take into consideration the endotherm before 60 °C.

The samples cooled down by natural convection and by the Cooling Press (Sect. 2) have been analysed. The eight samples' melting peak curves are displayed in Figure 5.

Since no differences were found between the different removal locations, curves have been split into two categories. Curves information below 60 °C will not be taken into account due to the post-crystallisation at room temperature.

Blue curves are always below pink ones in the temperature range between 60 °C and 85 °C. After 85 °C, blue curves are always above pink ones.

These results demonstrate that the cooling method has an impact on the encapsulant micro-structure. The faster the cooling the higher the number of big crystallites (melting peak of 93 °C) but the lower the number of middle size crystallites (between 60 °C and 85 °C).

So as to have a crystallinity value, the melting peak must be integrated. But since it varies due to post-crystallisation temperature, a last experiment has been performed. The two cooling configurations have been reproduced within the calorimeter. Samples were analysed right after the end of the cooling. Results are shown in Figure 6.

There is no peak around 50 °C on Figure 6. This result confirms again that the first melting peak around 50 °C is due to post-crystallisation. Figure 6 also confirms the tendency observed on Figure 5: the faster the cooling the bigger the crystallites. There is as many crystallites melting above 93.9 °C in both samples' types. But there is more crystallites melting around 93 °C when the fast cooling is used.

Results displayed in the upper center of Figure 6 are the temperature of the linear integration peak and the specific melting heat ($J.g^{-1}$). Using equation (1), the crystallinity of each sample have been calculated. It is of 13.39% and 13.24% for the ambient air cooling, and of 13.15% and 13.01% for the fast cooling. Considering the DSC precision and the arbitrary choice of the melting peak boundary temperatures, crystallinity differences are not significant.

Cristallinity is judged consistent. However, the fast cooling does generate a higher number of big crystallites.

This section has shown how the encapsulant crystallinity is influenced by the fast cooling delivered by the Cooling Press. The total crystallinity is equivalent for all the cooling methods. However, a higher number of large crystallites is generated during the fast cooling, and a fewer number of small to medium size crystallites. The encapsulant crystallinity is also dependant on the time spent at ambient temperature. A post-crystallisation have been brought to light.

4 Optical survey

The previous section has demonstrated that the micro-structure of the encapsulant is influenced by the cooling rate. This section is focusing on the optical consequences of this micro-structural change.

4.1 Method

Encapsulant samples have been removed from the instrumented modules presented in Section 2.1. Twelve 6×6 cm^2 samples of laminated encapsulant were used for the analysis. Three of them taken off from the module's center as shown in Figure 2 and the three others from the corner site location. This has been done for each cooling type which means six samples from the Cooling Press cooling and six other from the natural air convection cooling. Three different samples at each location and cooling type were taken to be statistically confident in the results. Measurements have been performed after two weeks at controlled room temperature. This allows to consider the samples' crystallinity stable during the measurements (less than one hour to perform the twelve samples).

Table 2. Integrated transmittance and reflectance relative difference (RD) between cooling with or without Cooling Press. The transmittance's order of magnitude is 84%. While the reflectance is of the order of 10.5%. Integration have been made between 300 nm and 1200 nm.

Samples' name	Transmittance RD (%)	Reflectance RD (%)
Center 1	−0.055	−0.671
Center 2	−0.030	−0.988
Center 3	−0.323	−0.829
Edge 1	0.024	−1.547
Edge 2	0.237	−0.348
Edge 3	−0.309	−0.053

The used spectrophotometer is a PerkinElmer. It uses an integrating sphere and the NREL reference air mass 1.5 spectra [6] for direct and diffuse solar spectrum. The outputted data are transmittance an reflectance for each wavelength. We integrated the results over the range 300 nm to 1200 nm wavelengths using the NREL reference air mass 1.5 spectra in order to have one value.

The same samples have also been analysed in a hazemeter. The hazemeter is a BYK haze-gard *i*. The Haze factor represents the material ability to diffuse uniformly the light in all direction. When the Haze factor is equal to 1, the result is a cloudy appearance of the material; equal to 0, material appears perfectly transparent.

Solar cells are hazy-dependent. They are sensitive to the light incident angle. Haze can enhance the cell' performances in homogenizing the distributed light rays on the cell surface. Two different haze factors, at consistent transmittance, will not have the same consequences on solar cells' performances. However, the impact of haze on cell's performances is lower than the impact of transmittance.

Samples were mere laminated encapsulant sheets, without glass layers. Since surface state is critical in optical measurements, uncertainties are set of the order of 2% [7].

4.2 Results

Results of the relative difference (RD) in transmittance and in reflectance are presented in Table 2. Relative difference is calculated as

$$RD = \frac{W_{ithout} - W_{ith}}{W_{ithout}} \times 100$$

where W_{ithout} refers to the cooling without Cooling Press and W_{ith} refers to the cooling with Cooling Press.

All the relative differences are below the 2% uncertainty explained in Section 3.1. It means that there is no significant difference for both transmittance and reflectance optical properties considering the cooling rate. Moreover, there is no significant difference between corner and center location.

Results for the Haze factor are presented in Table 3.

Table 3. Haze factor (%) and relative difference (RD) between cooling with or without the Cooling Press.

Samples' name	With CP	Without CP	RD (%)
Center 1	31.97	48.93	–34.7
Center 2	31.23	47.13	–33.7
Center 3	32.10	47.87	–32.9
Edge 1	30.20	46.17	–34.6
Edge 2	31.87	47.77	–33.3
Edge 3	30.50	46.20	–34.0

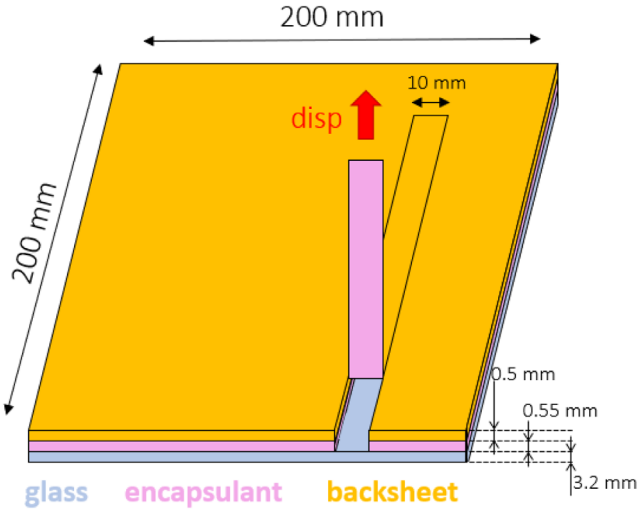

Fig. 7. Peeling test samples' architecture.

First, one can notice that this encapsulant is a very hazy material (EVA is below 10%). Reduction in the haze factor is clearly visible here when the cooling rate is higher. The mean reduction is about 34%. No noticeable differences are visible between corner and center locations.

This huge reduction in haze factor could be linked to the micro-structural differences seen in Section 3.2. Indeed, crystallites size have an effect on material haze factor [8]. And the only change made between the two experiments was the cooling rate.

This section has demonstrated the direct influence of the cooling rate on the haze factor through the crystallites' size distribution. Besides, it does not affect the total light transmittance nor reflectance.

5 Peeling bond strength

This section aims at describing and characterizing the influence of the Cooling Press on the bond between glass and encapsulant. Differences will be analysed just after lamination and over ageing. Simultaneously, it will be seen if pressure during the cooling step could have an influence over bonding.

Table 4. Peeling process manufacturing parameters. CP stands for Cooling Press.

Samples' number	With CP	Pressure during cooling (mbar)
4	No	0
4	Yes	200
4	Yes	385
4	Yes	770

5.1 Method

The method presented here uses a tensile test bench to measure the bond strength between encapsulant and glass. Sixteen samples were manufactured. Samples' architecture is given in Figure 7.

A backsheet is added to the encapsulant so as to be able to pull the encapsulant without deforming it. In order to have the same thermal history than the true process, samples were laminated with a second encapsulant layer and a second glass but separated by PTFE sheets to be able to remove these undesired parts.

Thermal and pressure history of the manufacturing process are presented in Figure 1. The different parameters used for the samples manufacturing are resumed in the following Table 4.

After lamination, samples are deburred and three 1 cm width testing strips are cut off with a ruler and a box cutter for each sample. These steps are manually realised and since peeling test are width sensitive, an important error source is the strip preparation.

Once testing strips are ready, a 180 peeling test is performed on a bi-column tensile test bench, INSTRON set 3360. Strips are pulled at 50 mm. min^{-1} while recording the strength. The peeled surface is 80 mm long. The obtained strength represent the peeling bond strength and characterise the bonding quality between glass and encapsulant. The usable value is the mean strength when a stationary regime is reached, here between 25 and 80 mm of the peeled surface length.

Once samples have been characterised, they are aged in a Damp Heat (DH) oven (+85 °C, 85% humidity content) for two periods of 500 h according to the norm IEC 61215 [9].

5.2 Results

Computed results are represented in Figures 8 and 9. On Figure 8, each column is the average result from three strips. There is four different samples per measurement point and per manufacturing type. Figure 8 shows scattered results.

Figure 9 presents the mean values between the four samples of each cooling pressure type.

Figure 9 shows the average value peeling force function of manufacturing process only. Each bar represents the mean of 12 strips. At initial time, the mean values were very closed. Considering the deviation factor, the starting point for all the manufactured processes can be considered as the same.

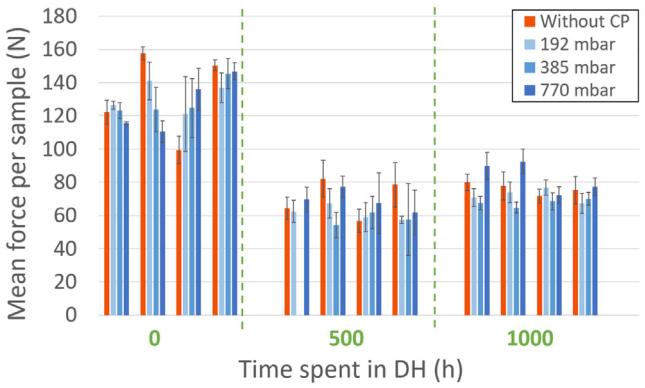

Fig. 8. Peeling test results per sample. Each column is the average of 3 strips. 4 samples were tested at each ageing point.

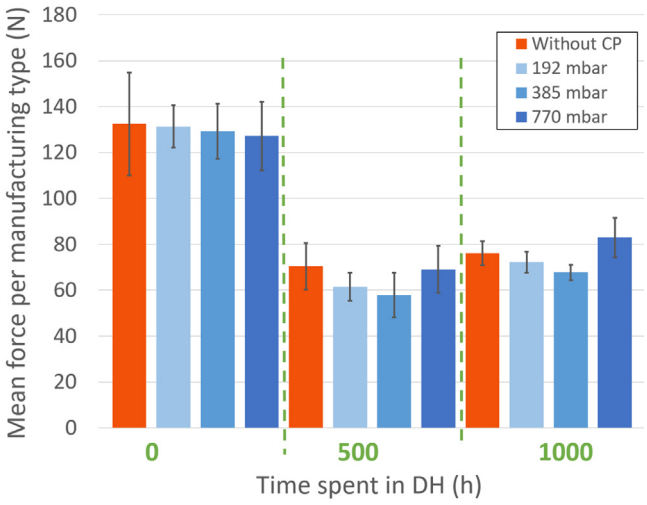

Fig. 9. Peeling test results per manufacturing process. Each column is the average of 12 strips.

Final results are not showing any clear differences between the groups. However it can be noticed the slightly increasing difference between the samples cooled at 770 mbar compared to the other ones. This slight difference need to be investigated at more than 1000 h of DH ageing. After 1000 h DH ageing, conclusion is still that no significant differences are visible.

Further studies are needed to investigate the previous trend with especially two more points – one between 385 and 770 mbar, and another over 770 mbar. These points can confirm/disprove the minimum peeling force between 385 and 770 bar that is taking shape here. Conducting the study to 2000 h or more is also needed to confirm the trend.

This section has demonstrated that applying pressure during cooling does not influence the glass-encapsulant bond strength after 1000 h of DH ageing. Results are valid for this TPO encapsulant only.

6 Influence of Cooling Press over ageing

This section aims at describing the influence of two accelerating ageing methods, Thermal Cycling (TC) and Damp Heat (DH), on the electrical components of a PV module. The present study is function of whether process uses the Cooling Press or not.

6.1 Method

Changing pressure and cooling rate when manufacturing modules may have an impact on PV modules' lifetime. The modified crystallinity (see Sect. 3.2) may modify the water diffusion in the module [10]. The pressure during cooling imposes shape on laminate, which can induce residual stresses.

That is why a study has been performed with six PV modules (700×600 mm^2) of 16 M2 mono-crystalline silicon PERC solar cells that had been cooled down with the Cooling Press (pressure of 256 mbar) and six others without Cooling Press. Same encapsulant and same manufacturing method than for the peeling test were used (see Sect. 5.1). It allows to be consistent between the experiments. Three of each kind were sent in Thermal Cycling (TC) (−40 °C to +85 °C in a 4 h cycle [9]) and three of each kind in Damp Heat (DH) (+85 °C and +85% of relative humidity) [9] accelerated ageing.

Modules have undergone 300 cycles in TC ageing, the normative recommendations is 200. They have been characterized at 0, 100, 200 and 300 cycles. In DH ageing, modules were aged during 1000 h, the normative recommendations. A characterization at 0 h, 500 h and 1000 h have been performed.

Characterization is constituted of a flash test and an electroluminescent test. A flash test is an analysis of the voltage and current of the whole module when illuminated with different irradiances, typically here 200, 600 and 1000 W.m^{-2}. This test allows to measure:

- $P_{\max}$ that represents the maximal power outputted during illumination and informs about the global state of the module.
- I_{SC} is the short-circuit current representing the maximum current able to circulate in the string of cells and characterizes the module ability to convert light into electricity.
- V_{OC} is the open circuit voltage and characterizes the cells state. It is influenced by the charges' recombination in the cell's bulk and on cell's surface.
- FF is the Fill Factor characterising the serial resistance of the whole electrical system.

Electroluminescent test is an analysis of the returned Infra-Red images of the cells when powered up with a current. This is the invert principle of solar cells that convert light into electricity. The returned image gives various information such as location of punctual defects, cells state (the more it shines, the better) and an idea of water diffusion in the module through cells or ribbons degradation. Input voltage was 20 V for a current of 9 A and an integration time of 1000 ms. Actually, the truly applied voltage is dependant of the cells' state, which is different for each module. The voltage was ranging from 14.5 V before ageing to 13.5 V after ageing. Cameras have the same settings for all pictures. All the images are post-processed with the same scale (light intensity maximum) to be consistent between them.

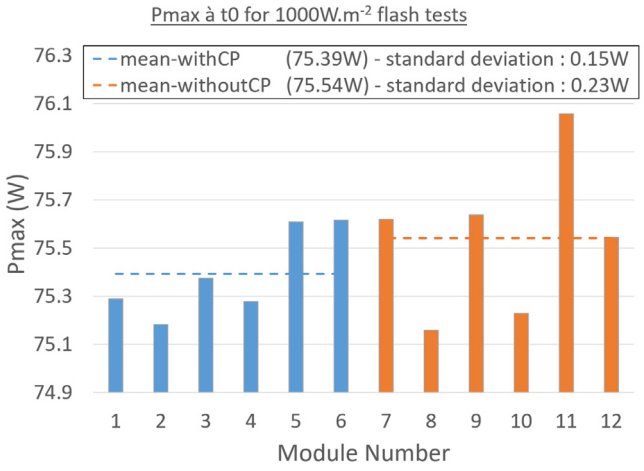

Fig. 10. Initial flash tests results for the twelve modules.

Before any measurement, the modules are left at controlled room temperature for more than half a day. Measurements are then performed in the same room. The measurement time is not sufficient to rise modules' temperature.

6.2 Results

Results of the initial time characterization − just after lamination − are presented in Figure 10. In blue are modules manufactured with Cooling Press, in orange without Cooling Press.

Considering the standard deviation, there is no significant difference between modules manufactured with and without Cooling Press at initial time. The mean maximum power is about 75.5 W when modules are illuminated at 1000 W.m^{-2}. However, comparing the standard deviation from the mean reveals that the process without Cooling Press is more irregular than the process using Cooling Press, respectively 0.23 W and 0.15 W.

6.2.1 DH ageing

After 500 h of DH ageing, flash test and EL have been performed. Results for flash test are presented in Figure 11 where ordinates are relative to the characterization made at initial time.

In blue colors are represented modules manufactured with Cooling Press and in red shades those without. Shapes and alignments represent the different irradiances − 200 W.m^{-2}, 600 W.m^{-2} and 1000 W.m^{-2}.

It can be seen in Figure 11 that the $P_{\max}$ loss is always worse for the solar panels that dealt with the Cooling Press. The $P_{\max}$ loss is about 3% for the two worst. Moreover, losses increase as light intensity decreases. Norm recommendation is to not exceed a loss of 5% for 1000 h of DH

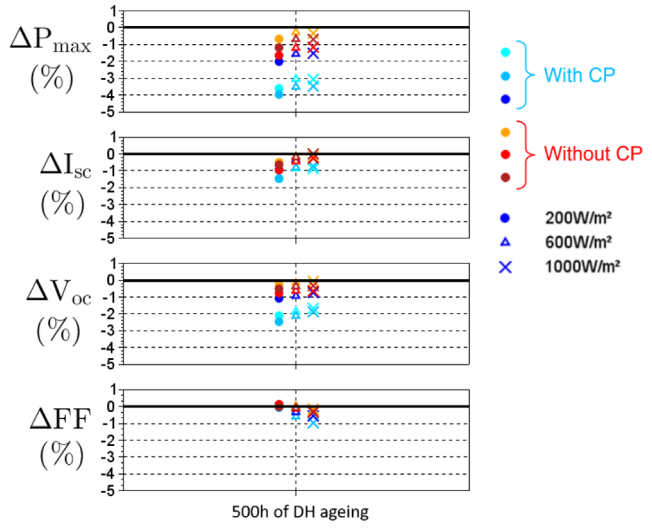

Fig. 11. PV modules power losses after 500 h of DH.

ageing. These losses in $P_{\max}$ are mostly due to V_{OC} losses − about 2% for the worst − and partially due to both I_{SC} and FF losses.

The V_{OC} depends on recombination in the solar cell. V_{OC} losses are traducing increasing recombination in cells [11,12]. Recombination can come from the cell's bulk or from cell's surface. The cell's bulk recombination ability is dependant on the material used. This suggests that the V_{OC} losses come from a deterioration of the cells' passivation layer, that has increased surfaces' recombination. Since, fast cooled modules are more damaged, the cells' passivation layer could have been damaged by the module's faster cooling or by the pressure imposed during cooling. The latter being the more likely to our knowledge. The fact that V_{OC} losses decrease with increasing light intensity would suggest that the serial resistance of the module is increased [13].

However, both I_{SC} and FF losses indicates that the shunt resistance is also increased and has a stronger influence than the serial resistance. This can be seen with the increasing loss of I_{SC} while decreasing light intensity. Shunt resistance can be related to the presence of water in the module.

A part of the results from the EL tests are presented in Figure 12.

It can be seen that indeed intensity of the worst module manufactured with the Cooling Press has decreased a lot, Figure 12a. Images have homogeneously lost in intensity strengthening the hypothesis of the cells passivation deterioration. No humidity deterioration can be detected.

From these results, it can be concluded that the use of the Cooling Press is not favourable towards modules using this TPO encapsulant and PERC cells in DH ageing conditions at 500 h. Results for 1000 h DH test are on going.

6.2.2 TC ageing

Both flash test and electroluminescent test were performed after 100, 200 and 300 TC to monitor degradation function of time. Results for flash test are presented in Figure 13 where ordinates are relative to the characterization made at initial time.

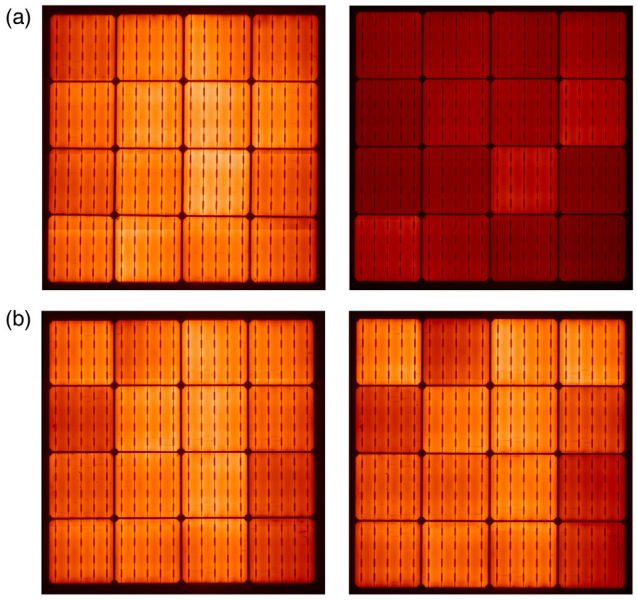

Fig. 12. Electroluminescent (EL) test results after 500 h DH for two out of the six modules that underwent DH tests. (a) EL test results at t_0 (left) and after 500 h DH (right) for the worst module manufactured with Cooling Press. (b) EL test results at t_0 (left) and after 500 h DH (right) for the worst module manufactured without Cooling Press.

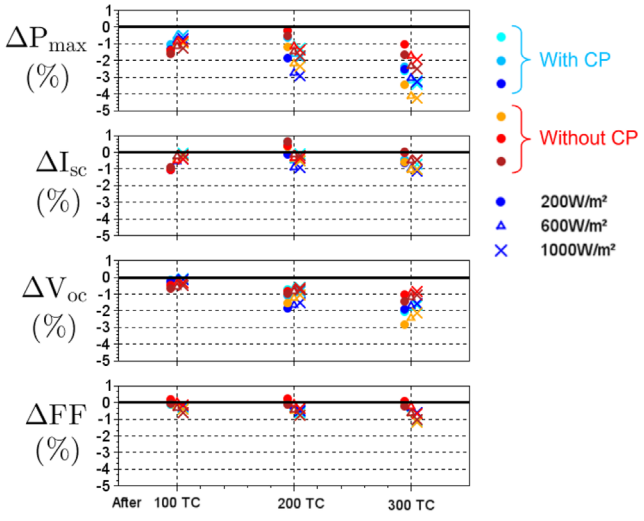

Fig. 13. Flash test losses compared to initial time for thermal cycling ageing.

In Figure 13 each group of three irradiances for one module are presented function of cycles' number. It can be seen in Figure 13 that no significant changes are visible for both I_{SC} and FF. It involves no change in the modules' optical properties. I_{SC} loss increases with light intensity indicating no shunt resistance rise. FF loss is related to a slight increase of the serial resistance. This is confirmed by V_{OC} losses increasing with light intensity. This can be

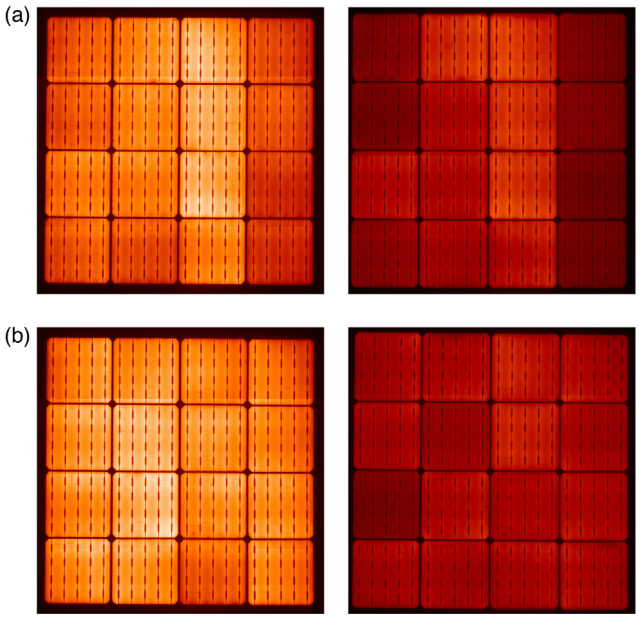

Fig. 14. Electroluminescent test results after 300 thermal cycles for two out of the six modules that underwent TC tests. (a) Electroluminescent test results at initial time (left) and after 300 TC (right) for the worst module manufactured with Cooling Press. (b) Electroluminescent test results at initial time (left) and after 300 TC (right) for the worst module manufactured without Cooling Press.

explained by an interconnection damage, which is normal in thermal cycling ageing.

At 300 TC, none of the six modules have lost more than 5% in $P_{\max}$ indicating that they all went into the norm [9]. Moreover, it can be seen that $P_{\max}$ losses are directly correlated with V_{OC} losses. Like previously, V_{OC} losses can be related to the passivation deterioration. This assumption is strengthened with the electroluminescent tests results (see Fig. 14). They show a uniform intensity loss, without any cell crack or hot-spot.

At 300 TC no differentiation between the fast cooling manufacturing and the slow one is detectable on the $\Delta P_{\max}$ mean. However, it seems that the three modules cooled by natural convection are more scattered than the three others, cooled with the Cooling Press. To be able to conclude or to see significant differences, we have decided to pursue TC ageing test until 500 cycles.

V_{OC} losses are more important for modules manufactured with the Cooling Press in damp heat conditions only. This phenomenon might be linked to the presence of humidity in the module or by the long exposure to 85 °C. PERC cells are not very sensitive to water. This could explain that EL tests did not revealed any degradation related to water while a certain amount of water was present in the module. This small amount of water could have increase cell's recombination and so V_{OC} losses. The lower temperature and humidity level of the thermal cycling ageing might not allowed water to access to the cells during the experimentation. This could explain the differences between the experiments' results.

This section has demonstrated that modules manufactured with Cooling Press were more sensitive to damp heat after 500 h than modules cooled by natural convection. No differentiation could be made after 300 TC between the cooling types.

7 Conclusion

This study has described a new cooling process: the Cooling Press. It has been shown that this cooling process is about five times quicker than a natural convection cooling. From this assessment, the guiding principle was to know whether the Cooling Press could have an influence on the semi-crystalline polymer encapsulant of a glass-glass PV module.

By DSC analysis, the encapsulant crystallinity has been estimated around 13%. The main differences have been found for the crystallites size scattering. The fast cooling process allows to form bigger crystallites but less medium size ones. This microstructual change finds an echo in the 34% decrease of the material haze factor, while the transmittance remains constant.

The bond between encapsulant and glass has also been assessed. After 1000 h of Damp Heat ageing, no significant difference was found between samples cooled by natural convection and samples cooled with the Cooling Press. No influence of the pressure during cooling could have been demonstrated.

Finally, the ageing behaviour of functional 16 cells PV modules have been discussed. It seems that the Cooling Press does not have any influence in Thermal Cycling ageing. On the contrary, Cooling Press seems to be harmful for PV modules when aged in a Damp Heat oven. Further experiments need to be carry out to confirm this trend.

One major defects of solar panels are crack propagation in cells. Crack propagation is due to both residual stresses in cells and the thermal expansion mismatch between materials. The influence of the Cooling Press over cells residual stress after lamination could be of the upmost interest.

The thermo-mechanical ageing behaviour of polymeric materials is also very interesting topic. It could help to understand degradation of solar panels. The influence of the cooling process over material thermo-mechanical properties ageing behaviour could also be investigated.

This study allowed to identify and quantify the consequences of the cooling process on PV modules properties. This is a step forward in the ageing behaviour understanding of solar panels. This study tried to help increasing modules' lifetime.

This work was supported by the French National Program "Programme d'Investissements d'Avenir – INES.2S" under Grant ANR-10-IEED-0014-01.

Author contribution statement

V. Meslier has performed all the experiments. V. Meslier, B. Chambion, A. Boulanger, I. Rahmoun conceived the study idea and analyzed all the data. V. Meslier wrote the article. B. Chambion and F. Chabuel reviewed the multiple versions of the manuscript. T. Bejat presented the article at WCPEC-8 (EU PVSEC 2022).

References

1. R. Androsch, Melting and crystallization of poly(ethylene-co-octene) measured by modulated d.s.c. and temperature-resolved X-ray diffraction, Polymer **40**, 2805 (1999)
2. B. Adothu, F.R. Costa, S. Mallick, Damp heat resilient thermoplastic polyolefin encapsulant for photovoltaic module encapsulation, Sol. Energy Mater. Sol. Cells **224**, 111024 (2021)
3. K. Agroui, G. Collins, J. Farenc, Measurement of glass transition temperature of crosslinked EVA encapsulant by thermal analysis for photovoltaic application, Renew. Energy **43**, 218 (2012)
4. Y.-L. Loo, K. Wakabayashi, Y.E. Huang, R.A. Register, B.S. Hsiao, Thin crystal melting produces the low-temperature endotherm in ethylene/methacrylic acid ionomers, Polymer **46**, 5118 (2005)
5. K. Agroui, G. Collins, Determination of thermal properties of crosslinked EVA encapsulant material in outdoor exposure by TSC and DSC methods, Renew. Energy **63**, 741 (2014)
6. NREL, Reference Air Mass 1.5 Spectra. 2005. url: https://www.nrel.gov/grid/solar-resource/spectra-am1.5.html (visited on 06/16/2022)
7. Y.J. Shen, Q.Z. Zhu, Z.M. Zhang, A scatterometer for measuring the bidirectional reectance and transmittance of semiconductor wafers with rough surfaces, Rev. Sci. Instrum. **74**, 4885 (2003)
8. R.J. Tabar, C.T. Murray, R.S. Stein, The effect of particle size on the haze of polymer films, J. Polym. Sci.: Polym. Phys. Edn. **21**, 831 (1983)
9. International Electrotechnical Commission, IEC-61215 – Terrestrial photovoltaic (PV) modules – Design qualification and type approval, International Standard (2021)
10. B. Fayolle, J. Verdu, Vieillissement physique des materiaux polymers, in *Techniques de l'Ingenieur*. AM 3150 01 (2005), p. 22
11. R.A. Sinton, A. Cuevas, Contactless determination of current-voltage characteristics and minority-carrier lifetimes in semiconductors from quasi-steady-state photoconductance data, Appl. Phys. Lett. **69**, 2510 (1996)
12. A. Cuevas, The Recombination Parameter J0, Energy Procedia **55**, 53 (2014)
13. G. Bunea, K. Wilson, Y. Meydbray, M. Campbell, D. De Ceuster, Low light performance of mono-crystalline silicon solar cells, in *2006 IEEE 4th World Conference on Photovoltaic Energy Conference* (2006), pp. 1312–1314

Cite this article as: Vincent Meslier, Bertrand Chambion, Amandine Boulanger, Ichrak Rahmoun, Fabien Chabuel, Timea Bejat, Effect of the cooling rate on encapsulant's crystallinity and optical properties, and photovoltaic modules' lifetime, EPJ Photovoltaics. **14**, 2 (2023)